

How Generalizable are Deepfake Detectors? An Empirical Study

Boquan Li, Jun Sun, and Christopher M. Poskitt

Abstract—Deepfake videos and images are becoming increasingly credible, posing a significant threat given their potential to facilitate fraud or bypass access control systems. This has motivated the development of *deepfake detection* methods, in which deep learning models are trained to distinguish between real and synthesized footage. Unfortunately, existing detection models struggle to generalize to deepfakes from datasets they were not trained on, but little work has been done to examine why or how this limitation can be addressed. In this paper, we present the first empirical study on the *generalizability* of deepfake detectors, an essential goal for detectors to stay one step ahead of attackers. Our study utilizes six deepfake datasets, five deepfake detection methods, and two model augmentation approaches, confirming that detectors do not generalize in zero-shot settings. Additionally, we find that detectors are learning unwanted properties specific to synthesis methods and struggling to extract discriminative features, limiting their ability to generalize. Finally, we find that there are neurons universally contributing to detection across seen and unseen datasets, illuminating a possible path forward to zero-shot generalizability.

Index Terms—Multimedia forensics, deepfake detection, generalization, empirical study.

I. INTRODUCTION

DEEPFAKES are manipulated videos or images created using deep learning algorithms [1]. The technology behind them has advanced to such a state that the best deepfakes are nearly indistinguishable from authentic footage. As deepfakes become more accessible and easier to create, they pose an increasing threat to individuals, organizations, and governments given their potential use for spreading misinformation, manipulating public opinion, committing fraud, or even bypassing access control systems [2].

In response to this growing risk, a considerable amount of research has been conducted on methods for detecting deepfakes, which can be categorized into two groups. The first group includes methods that rely on extracting specific features, such as visual artifacts [3], temporal information [4] and frequency information [5]. However, these detection methods are impractical in general, as such features are susceptible to objective factors such as environment conditions or image compression, and can be avoided by newer deepfake synthesis methods [6]. The second group includes methods based on deep learning, such as *MesoNet* [7] and *XceptionNet* [8], which classify real and deepfake videos based on their microscopic differences. These methods overcome the practical limitations of feature-specific detectors. However, given the

rapid development of deepfake technology, it is imperative that deepfake detectors are *generalizable*, meaning that their effectiveness is maintained across different deepfake datasets.

Research efforts that have attempted to make deepfake detectors generalizable can be broadly categorized into two groups. The first group of methods [9]–[13] achieve generalizable deepfake detection in *few-shot* settings, where techniques like transfer learning are applied to a few unseen deepfakes (i.e., examples from a different deepfake dataset than that initially trained on). While these methods report promising results, they will always be one step behind new deepfake datasets given that unseen examples are needed to generalize. The second group of methods [14]–[18], while primarily concerned with few-shot settings, also make tentative attempts in *zero-shot* settings, i.e., without requiring unseen deepfakes from other datasets. While the zero-shot setting is the most practical, unfortunately, these methods have had only limited success in it. Specifically, their results are only reported on certain unseen datasets [14]–[18], show limited effectiveness [14], [15], or are even contradicted in different research [16], [17]. This suggests that existing research efforts have not yet achieved successful generalizable deepfake detection.

While intuitively clear that we have not yet reached generalizable deepfake detection, we lack a systematic, comparative evaluation of the state-of-art. It would be useful to know which combinations of deepfake detection methods and model augmentation approaches lead to better generalizability. Additionally, it would be advantageous to gain insights into why deepfake detectors fail to generalize. For example, is it possible to extract information from their models to explain why zero-shot generalizability is challenging to achieve? Are there learnt features in the models that would be useful for achieving generalizability? To our knowledge, no empirical research has been undertaken to explore these factors in the context of deepfake detectors.

To address this, we conduct an empirical study by answering a series of research questions. Our study makes use of six deepfake datasets (focusing on the high-quality *Celeb-DF* and *Face2Face* datasets for initial training), five deepfake detection methods, and utilizes two model augmentation methods for generalizability. In particular:

- We study the extent to which current deepfake detectors generalize: is it true that state-of-the-art detectors generalize poorly? Through this question, we find that existing detectors are not generalizable in a zero-shot setting (with some mitigation possible in a few-shot one).
- Assuming deepfake detectors truly lack generalizability, are they learning ‘unwanted’ properties of deepfakes that fail to

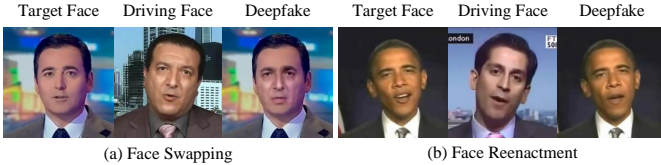


Fig. 1: Comparison of deepfake generation methods

characterize the essential differences between real and fake videos? Through this question, we find that detectors are learning unwanted properties specific to synthesis methods that interfere with their ability to generalize.

- Using interpretable artificial intelligence (AI) techniques, can we determine whether any of the features that detectors do extract are discriminative enough to classify real and fake videos? Through this question, we find that detectors do not extract discriminative features that support generalizability.
- We pivot away from extracted features and investigate deepfake detection models on a more granular level: in particular, are there neurons in the underlying neural networks that are contributing to the detection of deepfakes across both seen and unseen datasets? Through this question, we find the existence of such universal neurons, which suggests a possible new focus of future work aiming for generalizable zero-shot deepfake detection.

Furthermore, we provide a repository of deepfake detectors and datasets resulting from our study¹, which can serve as baselines or foundational blocks to support future research and applications.

II. BACKGROUND AND RELATED WORK

In this section, we review the necessary background on deepfake generation, deepfake detection, and generalizability of detectors. Following this, we compare our work against some related existing empirical studies on deepfakes.

A. Deepfake Generation

A deepfake is a synthetic video (or image) in which the face of a *target* individual is manipulated according to the face or expressions of a *driving face*. Current deepfake generation methods can be classified as performing either *face swapping* or *face reenactment*. In face swapping, the target provides the facial motions and expressions, but the face itself is replaced by that of the driving face. In face reenactment, however, the target retains their face but the motions are transformed into the ones provided by the driving face. Figure 1 [19] illustrates the difference between these two categories of methods.

Table I summarizes the current state-of-the-art deepfake synthesis methods across these two categories. The methods rely on a variety of underlying algorithms from image recognition and computer graphics (e.g., 3D model fitting), as well as deep neural networks (DNNs) such as autoencoders [20] and generative adversarial networks (GANs) [21].

Study scope. The key threat of these deepfake generation methods arises from the replacement of one human identity

with another: not only can this lead to social and political consequences, but there are also security implications, e.g., in bypassing face-based access control systems [2]. Note that we consider technologies for synthesizing non-existent images, such as image translation [24] or stable diffusion [25] algorithms, beyond the scope of our study, as the aforementioned threats only apply when considering the faces of real humans.

B. Deepfake Detection

Deepfake detection methods generally fall into one of two categories, based on *specific features* or *deep learning*. Table II summarizes the state-of-the-art deepfake detection methods across these two categories.

Specific feature analysis. The first category includes techniques that extract and analyse specific features (e.g., visual artifacts, temporal information and frequency information) for inconsistencies or search for abnormalities arising from deepfake generation. Korshunov et al. [26] explored the inconsistency between visual lip movements and audio speeches in deepfakes. Matern et al. [3] explored reflection details in eyes, teeth, and facial contours in deepfakes, and Yang et al. [27] extracted a full set of facial landmarks to estimate 3D head poses and detect abnormal poses. Similarly, Li et al. [28] explored the face warping step in deepfake creation and extracted the visual artifacts in face areas and their surrounding regions for classification. Agarwal et al. [29] focused on specific people and extracted facial expressions and movements to detect deepfake based on identity authentication. Additionally, Gu et al. [4] focused on the temporal information from video frames and aimed to find both spatial and temporal inconsistencies in deepfake videos. Liu et al. [5] combined spatial-image and phase-spectrum (frequency) features to capture artifacts for deepfake detection. However, these detectors have limitations in practical applications since specific features are susceptible to environment conditions (such as lights) or image compression, and can be avoided by newer deepfake methods [6].

Deep learning detectors. The second category utilizes DNNs such as convolutional neural networks (CNNs) [33] to classify real and deepfake videos based on microscopic-level features (i.e., pixel-level differences). Afchar et al. [7] proposed MesoNet, an efficient deepfake detector based on a lightweight network architecture. They also devised the improved MesoInception by appending a variant of the Inception module [34] to MesoNet. Tariq et al. [31] proposed three versions of ShallowNet, a method for detecting deepfakes generated by GANs, among which ShallowNet-V3 achieved the best performance. Additionally, Rossler et al. [19] and [35] [35] utilized the advanced XceptionNet [8] and EfficientNet [32] CNNs as Deepfake detectors, both of which achieved promising performance. Compared to specific-feature detectors, deep learning-based techniques are more practical since they focus on microscopic-level features (e.g., pixels) for classification, overcoming some of the limitations of visual artifact approaches mentioned earlier.

C. Generalizability of Deepfake Detectors

The deepfake detection methods we have discussed thus far typically focus on identifying deepfakes generated by one

¹We release our implemented datasets, deepfake detectors and codes in a Github repository. <https://github.com/boutiquelee/DeepfakeEmpiricalStudy>.

TABLE I: State-of-the-art deepfake generation methods

Method	Category	Algorithm	Project Page
FaceSwap	Face Swapping	Computer graphics	https://github.com/MarekKowalski/FaceSwap
DeepFake	Face Swapping	AutoEncoder	https://github.com/deepfakes/faceswap
FaceSwap-GAN	Face Swapping	AutoEncoder+GAN	https://github.com/shaoanlu/faceswap-GAN
Face2Face [22]	Face Reenactment	Computer graphics	http://niessnerlab.org/projects/thies2016face.html
Neural Textures [23]	Face Reenactment	GAN+Neural Textures	http://niessnerlab.org/projects/thies2019neural.html

TABLE II: State-of-the-art deepfake detection methods

Detector	Category	Feature	Classifier	Project Page
LipMovement [26]	Specific feature	Lip movements and speeches	IQM + SVM	https://gitlab.idiap.ch/bob/bob.report.deepfakes
VA-MLP [3]	Specific feature	Eyes, teeth and facial contours	MLP and LogReg	Unpublished
HeadPose [27]	Specific feature	Head poses	SVM	https://bitbucket.org/ericyang3721/headpose_forensic
FWA [28]	Specific feature	Face areas and surrounding regions	CNN	https://github.com/yuezunli/CVPRW2019_Face_Artifacts
WorldLeader [29]	Specific feature	Facial expressions and movements	SVM	Unpublished
STIL [4]	Specific feature	Spatial and temporal inconsistencies	CNN	https://github.com/Tencent/TFace
SPSL [30]	Specific feature	Spatial and phase-spectrum information	CNN	Unpublished
MesoNet [7]	Deep learning	Microscopic-level features	CNN	https://github.com/DariusAf/MesoNet
MesoInception [7]	Deep learning	Microscopic-level features	CNN	
ShallowNet [31]	Deep learning	Microscopic-level features	CNN	https://github.com/shahroztariq/ShallowNet
XceptionNet [8]	Deep learning	Microscopic-level features	CNN	https://github.com/shahroztariq/FaceForensics
EfficientNet [32]	Deep learning	Microscopic-level features	CNN	https://github.com/aaronchong888/DeepFake-Detect

TABLE III: State-of-the-art generalizable deepfake detection methods

Method	Category	Augmentation Strategy	Project Page
Forensictransfer [9]	Few-shot	Transfer Learning	Unpublished
ClassNSeg [10]	Few-shot	Multi-task Learning	https://github.com/nii-yamagishilab/ClassNSeg
CoReD [11]	Few-shot	Continual Representation Learning	https://github.com/alsgkals2/CoReD_Released
FReTAL [13]	Few-shot	Knowledge Distillation and Representation Learning	https://github.com/simrit1/FReTAL
TAR [12]	Few-shot	Weakly-supervised Learning	https://github.com/Clench/TAR_resAE
LTW [14]	Few-shot and Zero-shot	Meta-weight Learning	https://github.com/skJack/LTW
LAE [15]	Few-shot and Zero-shot	Active Learning	Unpublished
SLADD [16]	Few-shot and Zero-shot	Adversarial Augmentation	https://github.com/liangchen527/SLADD
OneRuleAll [17]	Few-shot and Zero-shot	Merge Learning and Transfer Learning	https://github.com/shahroztariq/CLRNet
SupCon [18]	Few-shot and Zero-shot	Supervised Contrastive Learning	https://github.com/xuyingzhongguo/deepfake_supcon

particular dataset. For detection methods to be practical in general, and for them to stay one step ahead of attackers, they must be able to generalize to identifying *any* upcoming deepfakes. Existing approaches that work towards this goal can be categorized as either *few-shot* or *zero-shot*: those in the former category require some additional deepfake examples from unseen datasets, whereas those in the latter do not. Table III summarizes the state-of-the-art generalization methods within these two categories.

Few-shot generalization. Generalization methods in this category take deepfake detection methods trained on one dataset, and generalize them by providing a few additional training examples from an unseen one. Cozzolino et al. [9] introduced a transfer learning approach that fine-tunes a detector to learn a forensic embedding for deepfake detection. Nguyen et al. [10] proposed a multi-task learning strategy that fine-tunes deepfake detectors in semi-supervised settings. Kim et al. [11] proposed a continual representation learning approach that performs domain adaptation between seen and unseen deepfakes. Similarly, Kim et al. [13] used both knowledge distillation and representation learning strategies to perform

domain adaptation on unseen deepfakes while minimizing ‘catastrophic forgetting’ (losing the model’s prior knowledge about deepfakes). Lee et al. [12] developed an autoencoder with residual blocks that performs weakly-supervised training on deepfake detectors. While these methods may achieve some generalization, they may not be practical in practice, since unseen deepfakes are often unavailable. Furthermore, it means that the detection method will always be one step behind an attacker that deploys a novel approach to deepfake generation.

Zero-shot generalization. As seen in Table III, existing works have predominantly focused on few-shot generalization. However, some authors have taken tentative steps to apply their methods in a zero-shot setting as well, i.e., in which (generalizable) deepfake detectors are trained without requiring examples from unseen datasets. In theory, zero-shot generalization is more practical, but existing efforts that reported promising results in few-shot settings have, unfortunately, only shown limited success in zero-shot ones.

In some research, results have only been reported on certain datasets or have only shown limited effectiveness. Sun et al. [14] proposed a meta-weight learning strategy that performs

domain adaptation between different datasets and achieved an accuracy of about 63% on unseen deepfakes. Du et al. [15] proposed a locality-aware autoencoder and an active learning framework, which achieved an accuracy of about 68% on a specific unseen dataset. Chen et al. [16] proposed an adversarial augmentation strategy, which achieved a passable performance, again, on a specific unseen dataset.

In other research, contradicting results have been reported. Tariq et al. [17] used merge learning and transfer learning strategies to fine-tune baseline detectors by augmenting multiple types of seen deepfakes, resulting in passable performance on specific unseen datasets. However, Xu et al. [18] reported that this strategy did not work on additional unseen datasets. To address this issue, they proposed a supervised contrastive loss strategy, which reported passable results on a specific dataset but showed poor performance on other ones.

D. Empirical Studies on Deepfakes

From the aforementioned work we have surveyed, it is intuitively clear that we have not yet reached (zero-shot) generalizable deepfake detection. We lack, however, a systematic evaluation of the state-of-the-art with respect to this goal. It would be useful to assess ‘where we are’ towards achieving generalization methods, why current methods fall short, and how generalizability might be achieved. Hence, the motivation of the empirical study proposed in this paper. While (to the best of our knowledge) this is the first such empirical study on the topic, there have been a number of other empirical studies on other aspects of deepfakes.

Several empirical studies have explored the impact of deepfakes in sociological domains. Vaccari et al. [36] investigated the contribution of deepfakes to online disinformation and highlighted the challenge they pose to online civic culture. Similarly, Gamage et al. [37] examined the social implications of deepfakes and proposed prospective management measures to mitigate their potential societal harms. In another study, Appel et al. [38] focused on political deepfakes and investigated the analytic thinking and political interests of citizens as predictors of correctly detecting deepfakes. Our empirical study differs by focusing on the generalizability of deepfake detectors within the technical domain only.

Other empirical studies have focused on the generation of non-existent objects or humans. Zhao et al. [39] studied the algorithmic mechanism of falsifying satellite images with non-existent landscape features. Liu et al. [40] studied entirely non-existent faces and investigated the transferability of GAN fingerprints for their detection. Yang et al. [41] also focused on non-existent faces and studied the network architecture attribution for their detection. In contrast to these studies, our work specifically focuses on deepfake methods that involve human identity replacements, such as face swapping and face reenactment, which pose actual threats to information security.

III. STUDY DESIGN

In this section, we present the design of our empirical study, including our research questions, datasets, baseline detectors, and implementation.

A. Research Questions

The overall goal of our study is to experimentally assess the extent to which state-of-the-art deepfake detectors can generalize, why current methods fail to generalize, and how generalizability might be achieved. In particular, we aim to answer the following research questions (RQs):

- RQ1 *Generalizability*. Do existing deepfake detectors generalize to deepfakes across different datasets?
- RQ2 *Unwanted Properties*. Do existing detectors learn deepfake properties that are unwanted for generalization?
- RQ3 *Discriminative Features*. Do deepfake detectors extract features that are discriminative enough for generalization?
- RQ4 *Contributing Neurons*. Do deepfake detection models have universally contributing neurons across seen and unseen datasets?

Through RQ1, we would like to systematically assess the extent to which current deepfake detection mechanisms can generalize in few-shot and (more importantly) zero-shot settings. In cases where detectors do not generalize, through RQ2, we wish to know whether detection models have learnt unwanted properties that interfere with the ability to characterize deepfakes. Through RQ3, we will apply AI interpretability techniques to assess the focus of deepfake detection models, i.e., whether they are extracting features that are discriminative enough for generalization. Finally, through RQ4, we assess deepfake detection models at a more granular level: through a causality-based analysis, can we identify neurons that contribute to the detection of seen and unseen deepfake datasets? The existence of such universally contributing neurons may support the prospect that future detection models can focus on generalizable features.

B. Dataset and Detector Selection

In order to answer our RQs, we require a representative selection of deepfake datasets and detectors, which we summarize in the following.

Deepfake datasets. For our study, we want to be able to assess generalizability across deepfakes generated by all of the state-of-the-art methods summarised in Table I. Thus, we selected the following datasets, which collectively cover all of the deepfake generation methods highlighted, and are frequently used to evaluate detectors in the literature.

- *FaceForensics++* [19], [42]. This benchmark consists of multiple sub-datasets, from which sets of 1000 deepfake videos were generated using each of the following synthesis methods: *FaceSwap* (FS), *DeepFake* (DF), *Face2Face* (F2F), and *NeuralTextures* (NT). The videos are provided in multiple levels of quality, of which we select the high-quality level (‘C23’) for our study. The dataset has been extensively used in evaluations, and has been cited approximately 1,500 times in the literature.
- *DeepFakeDetection* (DFD) [43]. In this work, Google AI proposed an improved version of the *FaceSwap*-GAN deepfake synthesis method, and released a dataset that was generated using it. The authors invited 28 actors to record 363 real videos, creating 3068 fake ones using this method. The dataset has been incorporated into the aforementioned

FaceForensics++ benchmark, indicating the community’s recognition of it as credible for evaluation.

- CELEB [44]. In this work, the authors proposed an improved version of the FaceSwap-GAN synthesis method and released two datasets resulting from it (CELEB-DF-V1 [6] and CELEB-DF-V2 [45]), which respectively contain 408 and 590 real videos as well as 795 and 5639 corresponding deepfakes; we utilize the latter in our study given the larger number of high-quality deepfake videos. CELEB is widely accepted as a dataset for evaluation in the community, and has been cited around 800 times in the literature.

Deepfake detectors. For our study, we selected every state-of-the-art deepfake detection method based on deep learning (in Table II, to be specific), which we summarize in the following. Note that we do not select any of the specific feature-based deepfake detection methods, because they already have practical limitations—before even considering generalization—as their requirement for stable features means that they fail to detect deepfakes reliably in newer datasets such as CELEB [6]. That is, the selected deep learning-based detectors are the most practical and important for assessing their potential for generalization.

- MesoNet, MesoInception [46]. Both detectors are based on CNN architectures, where MesoNet contains four convolutional and two dense layers, whereas MesoInception contains two inception [34], two convolutional, and two dense layers.
- ShallowNet [31]. Among the three CNN-based detectors proposed by the authors, we select the ShallowNet-V3 detection model as a baseline since it reports the best performance. This detector consists of eight convolutional and two dense layers.
- XceptionNet [19]. This CNN-based detector consists of two convolutional and 13 separable convolutional [8] layers, as well as one dense layer.
- EfficientNet [32]. There exist several versions of this network, and we adopt EfficientNet-B0 as one of our baseline detection models since it has been actually applied in practice [35]. This detector is based on a CNN architecture with two convolutional and seven MBCConv [47] layers, followed by a dense layer.

Model augmentation strategies. Recall from our reviews (Section II-C and Table III) that a number of works have investigated the use of model augmentation strategies to facilitate few-shot and (tentatively) zero-shot generalization. Following a review of the work, we selected two model augmentation strategies that: (1) can be applied to our selected deepfake detection methods; and (2) are associated with the most promising results. Based on these criteria, we selected transfer learning and merge learning, which achieved the most reasonable results across the works (in OneRuleAll [17], to be specific). To expand, transfer learning is a typical model augmentation strategy that is applied across several domains [48] in order to generalize the original model. One way to apply this strategy is by fine-tuning. Here, the weights of a pre-trained model (e.g., trained on one of our selected datasets) are frozen except for the last few layers, which are modified by extending knowledge from the original training set

TABLE IV: Implemented deepfake detectors

Detector	Architecture	Training Dataset		Fine-tuning	Original Accuracy (%)	Average Accuracy (%)
		Original	Augmented			
XceptionNet1	2-Conv 12-SeparableConv 1-SeparableConv 1-Dense	CELEB	—	—	99.10	95.93
XceptionNet2		CELEB	CELEB, FS, NT	Transfer	98.45	
XceptionNet3		CELEB	CELEB, FS, NT	Merge	93.60	
XceptionNet4		F2F	—	—	96.15	
XceptionNet5		F2F	F2F, FS, NT	Transfer	93.35	
XceptionNet6		F2F	F2F, FS, NT	Merge	94.90	
MesoInception1	2-Inception 2-Conv 2-Dense	CELEB	—	—	97.70	95.23
MesoInception2		CELEB	CELEB, FS, NT	Transfer	96.50	
MesoInception3		CELEB	CELEB, FS, NT	Merge	89.05	
MesoInception4		F2F	—	—	97.60	
MesoInception5		F2F	F2F, FS, NT	Transfer	96.35	
MesoInception6		F2F	F2F, FS, NT	Merge	94.15	
MesoNet1	4-Conv 2-Dense	CELEB	—	—	97.60	94.69
MesoNet2		CELEB	CELEB, FS, NT	Transfer	96.85	
MesoNet3		CELEB	CELEB, FS, NT	Merge	85.50	
MesoNet4		F2F	—	—	97.35	
MesoNet5		F2F	F2F, FS, NT	Transfer	96.20	
MesoNet6		F2F	F2F, FS, NT	Merge	94.65	
EfficientNet1	1-Conv 7-MBCConv 1-Conv 1-Dense	CELEB	—	—	88.45	81.35
EfficientNet2		CELEB	CELEB, FS, NT	Transfer	88.15	
EfficientNet3		CELEB	CELEB, FS, NT	Merge	79.05	
EfficientNet4		F2F	—	—	78.50	
EfficientNet5		F2F	F2F, FS, NT	Transfer	76.80	
EfficientNet6		F2F	F2F, FS, NT	Merge	77.15	
ShallowNet1	8-Conv 2-Dense	CELEB	—	—	85.40	77.70
ShallowNet2		CELEB	CELEB, FS, NT	Transfer	71.15	
ShallowNet3		CELEB	CELEB, FS, NT	Merge	73.20	
ShallowNet4		F2F	—	—	88.85	
ShallowNet5		F2F	F2F, FS, NT	Transfer	76.60	
ShallowNet6		F2F	F2F, FS, NT	Merge	71.00	

or by learning knowledge from new ones (e.g., as in the few-shot approach). Merge learning, in contrast, is a more extreme strategy for generalization since it fine-tunes all the layers of a detection model using one or more additional datasets.

C. Implementation

To facilitate our experiments, we trained 30 deepfake detectors using the models and datasets identified in Section III-B. In particular, for each of the five CNN architectures, we trained a detector on the CELEB dataset and another on the F2F data extracted from FaceForensics++. For each of the resulting detectors, we augmented (copies of) the models using either transfer or merge learning based on additional samples from the training set as well as samples from unseen ones (FS, NT). Note that CELEB and F2F are selected for model training, since they respectively belong to categories of face swapping and face reenactment, and are generated based on deep learning and computer graphics methods, which allows for fair and comprehensive evaluations (the selection of FS and NT for fine-tuning follows the same considerations). Table IV summarizes the resulting detectors, and we present more details on their training in the following.

First, as a pre-processing step, we utilized a face recognition project [49] to extract 10 frames from each video in our selected datasets, align and crop their facial regions, and save the cropped images in PNG format with a size of 256×256 .

Next, to train the ‘original’ deepfake detectors such as MesoNet1 and MesoNet4, i.e., without any model augmentation, we used a training set of 16,000 images from the (respective) original datasets. To further train the fine-tuned detectors (such as MesoNet2 and MesoNet3), the augmented training set consisted of 2,000 additional images from the original dataset as well as 2,000 from FS and NT. When performing transfer learning, we fine-tuned the last two

function layers of the original deepfake detectors, or other parts of the architecture that contain significant features for classification (indicated in **bold** in Table IV).

Each deepfake detector in the table was trained based on an Adam [50] optimizer with $\beta_1 = 0.9$ and $\beta_2 = 0.999$. The learning rate for each of the `MesoNet` and `MesoInception` detectors was 10^{-3} , whereas for the remaining detectors it was 5×10^{-5} . Moreover, the original and fine-tuned detectors were respectively trained for 100 and 50 epochs, and the best-performing parameters are adopted (instead of the last-epoch ones). All training and evaluation were conducted on a server with an Intel Core i9-9900 3.1GHz CPU, 128GB memory, and two NVIDIA GeForce RTX 2080Ti graphics cards.

Table IV also shows the accuracy of each trained detector. The ‘original accuracy’ was evaluated based on testing images extracted from CELEB or F2F respectively. For our study, each testing dataset is composed of 2,000 images that are fully independent of the training ones. We remark that each of our training and testing datasets consists of 50% real and 50% deepfake images. As seen in the table, most deepfake detectors have promising accuracy, although it is poor (below 80%) for a number of the fine-tuned ones, e.g., `ShallowNet2`. In these cases, fine-tuning inevitably impacted the original performance of the models, since learning new knowledge unavoidably weakens their attention to the features in original datasets.

IV. EMPIRICAL STUDY

In this section, we describe the experiments designed to answer our four RQs (Section III-A), present the results, and summarize our findings.

A. Generalizability of Deepfake Detectors (RQ1)

Experiment. Recall our goal to determine the extent to which existing deepfake detectors generalize to deepfakes across datasets other than those they trained on. To achieve this, we took each of the 30 implemented deepfake detectors described in Section III-C and evaluated their accuracy on the unseen datasets described in Section III-B, in particular, FS, NT, DF, and DFD. Note that although a number of samples from FS and NT have participated in the fine-tuning of partial detectors (e.g., `MesoNet2` and `MesoNet3`), we still consider the independent testing images from the two datasets as unseen ones, since this is a general ‘few-shot’ setting.

Results. We present our evaluation results in Table V.

Measure of generalizability. As the rightmost columns in the table, we measure the generalizability of a deepfake detector by computing its performance degradation, i.e., the difference between its original accuracy (i.e., on the original testing dataset) and the average accuracy it achieved across different unseen datasets. Note that for performance degradation, lower values indicate better generalizability, whereas higher values indicate that the respective detectors generalize poorly to the given unseen datasets.

Result analysis. First, we observe that most of these detectors (at ranks #8–30) generalize poorly, with all but the top seven of our detectors seeing a performance degradation of over 20 percentage points (and as many as 44.76 percentage points

TABLE V: Generalizability of detectors to unseen datasets

Rank	Detector	Original Accuracy (%)	Unseen Dataset					Degradation (% points)
			Accuracy (%)					
			FS	NT	DF	DFD	Average	
1	<code>ShallowNet6</code>	71.00	79.50	75.60	56.20	52.10	65.85	5.15
2	<code>ShallowNet2</code>	71.15	75.60	70.85	53.60	51.75	62.95	8.20
3	<code>ShallowNet3</code>	73.20	75.60	71.40	53.95	55.60	64.14	9.06
4	<code>ShallowNet5</code>	76.60	78.55	77.75	57.20	55.85	67.34	9.26
5	<code>EfficientNet6</code>	77.15	75.05	76.15	55.30	46.15	63.16	13.99
6	<code>MesoNet3</code>	85.50	75.50	76.10	65.95	61.45	69.75	15.75
7	<code>EfficientNet3</code>	79.05	67.70	66.35	63.05	50.35	61.86	17.19
8	<code>MesoInception3</code>	89.05	76.25	71.05	59.50	56.95	65.94	23.11
9	<code>EfficientNet5</code>	76.80	51.25	54.30	56.30	49.40	52.81	23.99
10	<code>XceptionNet3</code>	93.60	80.75	76.35	63.90	55.10	69.03	24.58
11	<code>XceptionNet6</code>	94.90	83.95	83.40	58.50	53.25	69.78	25.13
12	<code>MesoNet6</code>	94.65	77.80	76.90	60.95	57.95	68.40	26.25
13	<code>EfficientNet4</code>	78.50	49.10	53.90	55.85	48.80	51.91	26.59
14	<code>MesoInception6</code>	94.15	82.05	78.25	56.45	52.70	67.36	26.79
15	<code>ShallowNet1</code>	85.40	58.05	50.20	54.90	49.60	53.19	32.21
16	<code>ShallowNet4</code>	88.85	53.50	53.35	58.45	55.15	55.11	33.74
17	<code>EfficientNet2</code>	88.15	50.30	50.40	58.25	52.60	52.89	35.26
18	<code>EfficientNet1</code>	88.45	51.95	49.80	58.70	51.95	53.10	35.35
19	<code>XceptionNet5</code>	93.35	60.00	62.55	56.70	47.25	56.63	36.73
20	<code>MesoNet5</code>	96.20	64.55	62.40	56.75	53.55	59.31	36.89
21	<code>MesoInception5</code>	96.35	57.45	60.60	60.50	55.50	58.51	37.84
22	<code>MesoNet2</code>	96.85	57.55	58.35	60.80	55.65	58.09	38.76
23	<code>MesoInception2</code>	96.50	54.65	55.25	56.85	51.60	54.59	41.91
24	<code>MesoNet1</code>	97.60	51.15	52.30	61.80	55.75	55.25	42.35
25	<code>XceptionNet4</code>	96.15	48.80	55.75	57.30	50.80	53.16	42.99
26	<code>MesoNet4</code>	97.35	54.55	52.20	56.00	54.35	54.28	43.08
27	<code>MesoInception4</code>	97.60	50.00	53.35	59.10	53.95	54.10	43.50
28	<code>MesoInception1</code>	97.70	52.80	52.10	57.10	51.90	53.48	44.23
29	<code>XceptionNet2</code>	98.45	55.25	51.15	56.80	53.45	54.16	44.29
30	<code>XceptionNet1</code>	99.10	54.60	50.95	57.00	54.80	54.34	44.76

for `XceptionNet1`). Upon inspecting the accuracy of our detectors on specific unseen datasets, we observe that most of them are below 70%, with multiple results close to 50% which can be considered as good as a random guess. For example, the rank #30 `XceptionNet1` achieves only 54.60% accuracy on FS, 50.95% on NT, 57.00% on DF and 54.80% on DFD. Furthermore, although the detectors at ranks #1–7 achieve passable performance degradation (below 20 percentage points), their accuracies on the fully unseen datasets remain below 70%. For example, `MesoInception3` achieves accuracies of 59.50% and 56.95% on DF and DFD. Such results confirm the inability of these detectors to generalize in zero-shot settings.

Second, we observe that the detectors at ranks #1–7 achieve performance degradation below 20 percentage points, which is more remarkable than those at ranks #8–30. To further observe their specific accuracy results, the accuracy of several detectors (not limited to the ones at ranks #1–7) is over 70% on the unseen FS and NT datasets. For example, on FS and NT, `ShallowNet6` achieves accuracies of 79.50% and 75.60%, and `MesoInception3` achieves accuracies of 76.25% and 71.05%. Recall that these detectors were augmented using merge learning, in which a total of 1000 deepfake images from FS and NT were used for fine-tuning. This suggests that these detectors can generalize to particular unseen datasets with the help of a few unseen deepfakes.

In general, these results are consistent with those previously published results on few-shot and zero-shot generalizability (Section II-C).

Finding 1: Existing deepfake detectors are not generalizable in zero-shot settings, and the performance degradation can be mitigated in few-shot settings.

B. Learning Unwanted Properties (RQ2)

Given that deepfake detectors do not generalize except in some few-shot settings (Section IV-A), it is intuitive that detectors may have learnt certain unwanted properties rather than those intrinsic ones in deepfakes. For example, if deepfake detectors are learning properties that pertain to specific synthesis methods or human identities, this might interfere with learning the essential difference between real and fake samples. We explore this intuition in RQ2.

Experiment. First, we selected the detectors trained on CELEB-DF-V2 (Section III-C), and then evaluated them against CELEB-M, a specialized dataset consisting of real and deepfake images from CELEB-DF-V1 [6]. The process of creating CELEB-M follows the same settings as the testing datasets implemented in Section III-C. As deepfakes in this dataset were synthesized using the same method as those in the detectors’ training set, the intention was that a detector learning *method-specific* properties of deepfakes would exhibit better generalizability on CELEB-M, compared with the performance on the other unseen ones.

Second, we selected the detectors trained on F2F, and then evaluated them against FS-I and NT-I. Different from FS and NT, FS-I and NT-I are two specialized datasets where the real and deepfake images share the same human identities as the ones in F2F. The intention was that a detector learning *human identity-specific* properties of deepfakes would exhibit better generalizability on FS-I and NT-I, compared with the performance on other unseen datasets.

Intuition. For those detectors originally showing poor generalizability, if some abnormal (good) generalizability results are observed on any specialized datasets, they must have learnt certain properties of those deepfake detection methods. Following this intuition, the above experiments were conducted based on those detectors exhibiting the poorest generalizability (performance degradation over 30%) in Table V.

Results. We present the results of our evaluation on CELEB-M in Table VI, and the ones on FS-I and NS-I in Table VII. For convenience, the two tables repeat the average accuracy and degradation on the FS, NT, DF, and DFD datasets. They also show the average accuracy of detectors on the specialized datasets, as well as the degradation in performance when compared to the original accuracy.

Measure. In the rightmost columns in the two tables, we measure a deepfake detector’s generalizability change (from unseen to specialized datasets) by computing its performance degradation difference between the two groups of datasets. Note that for the degradation difference, a higher value indicates *less degradation* (and thus better generalizability) on CELEB-M (or FS-I and NT-I) compared to the other unseen datasets; negative values indicate that the generalizability gets worse on the specialized datasets.

Result analysis. First, in Table VI we observe that the difference in degradation is over 10 percentage points for the top six deepfake detectors in the table (e.g., 24.95% for MesoNet1), suggesting that their generalizability is significantly improved when encountering the CELEB-M dataset. For the other detectors at ranks #7-9, although the differences in degradation are not remarkable, they still perform better

TABLE VI: Accuracy of detectors on an unseen dataset synthesized by the same method as the training set

Rank	Detector	Original Accuracy (%)	Unseen Dataset					Specialized Dataset			Degradation Difference (%)	
			Accuracy (%)					Degradation (% points)	Accuracy (%)			Degradation (% points)
			FS	NT	DF	DFD	Average		CELEB-M	(% points)		
1	MesoNet1	97.60	51.15	52.30	61.80	55.75	55.25	42.35	80.20	17.40	24.95	
2	XceptionNet1	99.10	54.60	50.95	57.00	54.80	54.34	44.76	76.05	23.05	21.71	
3	XceptionNet2	98.45	55.25	51.15	56.80	53.45	54.16	44.29	75.15	23.30	20.99	
4	MesoInception1	97.70	52.80	52.10	57.10	51.90	53.48	44.23	74.25	23.45	20.78	
5	MesoNet2	96.85	57.55	58.35	60.80	55.65	58.09	38.76	77.00	19.85	18.91	
6	MesoInception2	96.50	54.65	55.25	56.85	51.60	54.59	41.91	71.75	24.75	17.16	
7	ShallowNet1	85.40	58.05	50.20	54.90	49.60	53.19	32.21	62.85	22.55	9.66	
8	EfficientNet2	88.15	50.30	50.40	58.25	52.60	52.89	35.26	60.70	27.45	7.81	
9	EfficientNet1	88.45	51.95	49.80	58.70	51.95	53.10	35.35	60.55	27.90	7.45	

TABLE VII: Accuracy of detectors on unseen datasets containing the same human identities as the training set

Rank	Detector	Original Accuracy (%)	Unseen Dataset					Specialized Dataset			Degradation Difference (%)		
			Accuracy (%)					Degradation (% points)	Accuracy (%)			Degradation (% points)	
			FS	NT	DF	DFD	Average		FS-I	NT-I			Average
1	ShallowNet4	88.85	53.80	53.35	58.45	55.15	55.11	33.74	66.95	61.15	64.05	24.80	8.94
2	XceptionNet5	93.35	60.00	62.55	56.70	47.25	56.63	36.73	64.40	61.00	62.70	30.65	6.08
3	XceptionNet4	96.15	48.80	55.75	57.30	50.80	53.16	42.99	57.80	55.65	56.73	39.43	3.56
4	MesoInception4	97.60	50.00	53.35	59.10	53.95	54.10	43.50	53.90	53.85	53.88	43.73	-0.22
5	MesoNet4	97.35	54.55	52.20	56.00	54.35	54.28	43.08	55.25	52.35	53.80	43.55	-0.48
6	MesoNet5	96.20	64.55	62.40	56.75	53.55	59.31	36.89	59.80	57.25	58.53	37.68	-0.79
7	MesoInception5	96.35	57.45	60.60	60.50	55.50	58.51	37.84	54.50	56.15	55.33	41.03	-3.19

accuracy and generalizability on CELEB-M compared to other unseen datasets. For example, the rank #7 ShallowNet1 achieves an accuracy of 62.85% on CELEB-M that is higher than the ones on FS, NT, DF, and DFD (58.05%, 50.20%, 54.90% and 49.60%). Overall, these results can indicate that using the same synthesis method to generate the unseen dataset leads to better accuracy, suggesting that the detectors have learnt (unwanted) method-specific properties of deepfakes.

Second, in Table VII, we observe that the difference in degradation is below 10 percentage points for all the detectors (e.g., 8.94% for ShallowNet4), indicating little-to-no impact when using the same human identities in the specialized datasets. The bottom four detectors present negative values (e.g., -3.19% for MesoInception5), and their absolute values are also below 10 percentage points, which also confirms FS-I and NS-I are not unique compared to other unseen datasets. Overall, these results suggest that these deepfake detectors have not learned human-identity features.

In general, these results are consistent with the perception that learning properties specific to synthesis methods lead to generalization issues across datasets. In practice, we do not want detectors to focus on such properties, but rather the intrinsic characteristics of deepfakes in general.

Finding 2: Deepfake detectors are learning unwanted features specific to synthesis methods, and human identities do not appear to have a significant effect on generalizability.

C. Learning Discriminative Features (RQ3)

The above experiments for RQ2 (Section IV-B) suggest that deepfake detectors may be learning (unwanted) properties that are specific to particular deepfake generation methods, which may be impeding the ability of detectors to generalize to unseen datasets generated using different methods. In RQ3, we explore the other side of the coin: using interpretable AI techniques, can we find any features that detection models are learning that

may be discriminative enough to distinguish real and deepfake images *in general*?

To answer this question, we applied Gradient-weighted Class Activation Mapping (Grad-CAM) [51], a popular technique used in computer vision for helping to interpret neural networks [52].

Background. Grad-CAM achieves neural network interpretation by generating a heatmap that highlights the regions of the input image that contributed the most to the neural network’s decision. In our case, the inputs of Grad-CAM are deepfake detectors and test deepfakes, and the outputs are heatmaps that visualize the regions of the test deepfakes that highly contributed to the decision of ‘real’ or ‘fake’, based on class prediction scores.

Specifically, given a detector and a desired class (e.g., ‘fake’), a deepfake input is first propagated through the detector’s Conv layers and then through task-specific computations to obtain a raw score for the class. The gradients are set to 1 for the desired class and 0 for the other. Then, the signal is backpropagated to the rectified convolutional feature maps, which are combined to compute a coarse location heatmap (i.e., the detector makes particular decisions based on the coarse location). Finally, the coarse heatmap is pointwise-multiplied using guided backpropagation to obtain the final heatmap.

Visualization Experiments. We first conduct a visualization experiment to preliminarily observe the features for deepfake detection. Specifically, we implemented Grad-CAM based on the Tf-Explain project [53] and applied it to our deepfake detectors (Section III-C) on the unseen FS, NT, DF, and DFD datasets. We used the settings recommended in [51], i.e., to visualize the contributing features in the last convolutional layer of each deepfake detector, since such layers are close to output layers and involve relatively complete features for classification. Moreover, instead of superimposing heatmaps on the original images, we generated pure heatmaps based on the applyColorMap function in OpenCV [54] to facilitate the analysis of visualized features.

Result analysis. Figure 2 presents a few example feature visualization results, where colors of higher intensity (such as red) indicate higher contributions towards the neural network’s deepfake classification decision. Ideally, the contributing features would be located in certain fixed facial regions, suggesting that detectors have extracted features that discriminate between real and fake in human faces. However, as the examples in the figure illustrate, the visualized features are scattered across different regions of the deepfakes, including foreheads, eyes, mouths, and even backgrounds, suggesting that they are not consistently extracting discriminative features.

Quantitative Experiments. We would like to provide a preliminary exploration through the above visual results, and then conduct quantitative experiments to further explore the discriminative features in deepfakes.

Intuition. We quantitatively measured the similarity between heatmaps generated by deepfake detectors that have the same architectures and training sets (e.g., MesoNet1, MesoNet2, MesoNet3). That is, these detectors are ‘congenetic’, i.e., they derive from the same original detector and are constructed with certain model augmentations. Ideally, given a test deepfake,

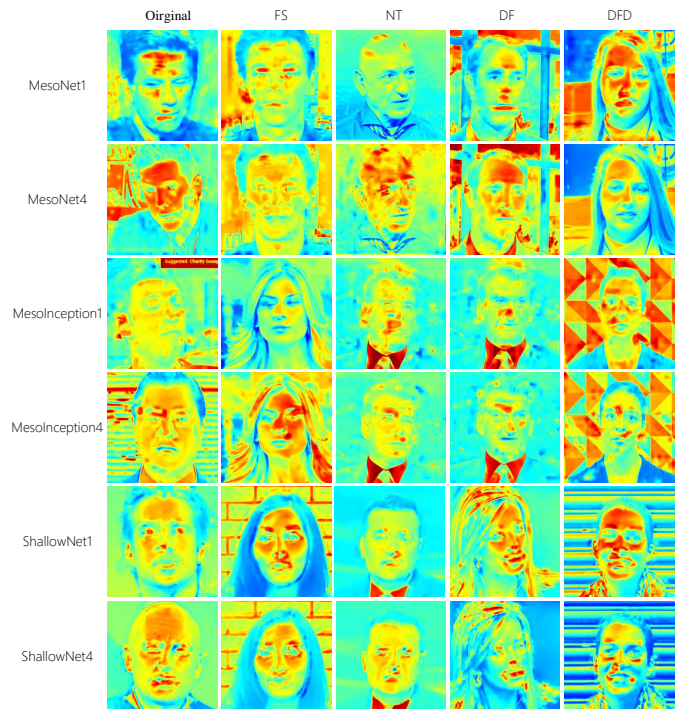


Fig. 2: Heatmaps visualizing the regions contributing to deepfake detectors’ classification decisions across datasets: the intense and cool colors (such as red and blue) indicate high and low contributions respectively

such detectors could focus on similar features on it, otherwise, their extracted features could be ‘unrestrained’ and are not discriminative enough for classification.

In particular, we applied Structural Similarity (SSIM) [55] for this purpose. SSIM evaluates the similarity between images based on three aspects [55], i.e., luminance, contrast and structure. These values are combined into a similarity score ranging from 0 to 1, where 1 indicates identical images. SSIM is selected since luminance and contrast are sensitive to the brightness of images, which matches the characteristics of heatmaps. For each group of detectors, we applied them to 1000 deepfakes from each of the unseen datasets, generated heatmaps accordingly, and measured their SSIM. Usually, 0.9 is applied as an SSIM threshold to determine whether test images have high similarity; 0.7 is the threshold to determine whether test images are dissimilar [55]; and values between 0.7 and 0.9 indicate low amounts of similarity.

Result analysis. We present our quantitative results in Figure 3. In the figure, we observe that the SSIM of most groups of heatmaps is below 0.7 (the red columns) indicating that most heatmaps are dissimilar, despite generating them in groups of detectors with similar underlying architectures. As exceptions, a few groups of heatmaps show higher SSIM values (between 0.7 and 0.8; orange columns) indicating low amounts of similarity. For example, in Figure 3 (b), 66.7% of the heatmaps generated for the original testing set (F2F) have SSIM values between 0.7 and 0.9. Such values are reasonable in the original testing set where the extracted

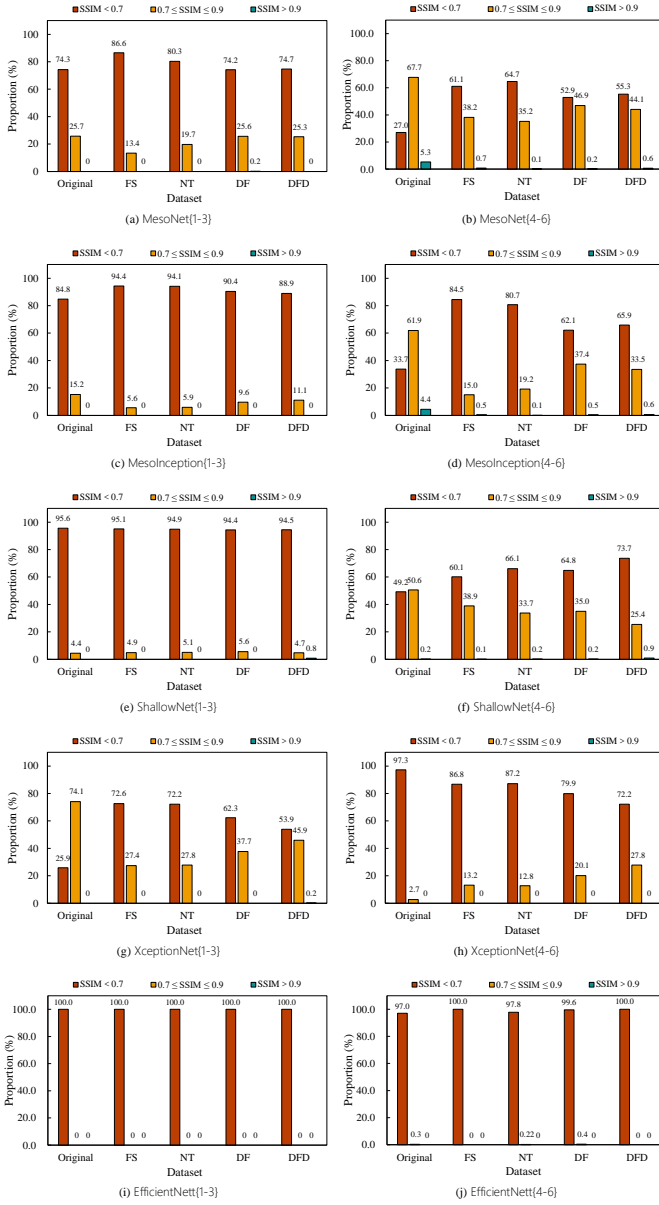


Fig. 3: Similarity (SSIM) of heatmaps generated by groups of deepfake detectors on unseen datasets

features are likely to be more similar than those in unseen ones. Nonetheless, across the ten histograms, very few groups of histograms achieved SSIM values above 0.9 (green bars). Recall that these ‘congenetic’ detectors should have extracted similar features from the same testing deepfakes, and the contrast results confirm that the contributing features are not discriminative for generalization.

Finding 3: Deepfake detectors are extracting unrestrained features that are not discriminative enough for generalizable detection.

D. Contributing Neurons (RQ4)

The results thus far suggest a fundamental challenge must be overcome before generalizable (zero-shot) deepfake detection

can become a realistic prospect. In this RQ, we approach the question of generalizability from a more granular perspective, asking whether detection models have universally contributing *neurons* across seen and unseen datasets. Rather than exploring *features* from input data as in RQ2 and RQ3, contributing neurons may facilitate a new way to identify features for classification. If such neurons exist, they may eventually provide a foundation for building generalizable deepfake detectors.

In a neural network, some neurons may contribute more to the classification result than others, a fact that has been exploited in other work to achieve, e.g., neural network repair [56]. Inspired by this work, we propose a *causality-based* method to analyze deepfake detection models so as to identify contributing neurons that are causally associated with classifying a testing image as real or fake.

Background. Specifically, we identify the contributing neurons by interpreting a deepfake detector as a Structural Causal Model (SCM), which is a significant causality analysis model that has been applied to multiple neural network interpretation tasks, e.g., [46], [57]. Formally, an SCM is defined as follows [58]:

Definition 1 (Structural Causal Model (SCM)). A *structural causal model (SCM)* is a four-tuple $C(Y, K, f, P_k)$, where Y and K are finite sets of endogenous and exogenous variables respectively, f is a set of functions $\{f_1, f_2, \dots, f_n\}$, and P_k is a probability distribution over K . Each function of f represents a causal mechanism such that $\forall y \in Y, y_i = f(Pa(y_i), k_i)$, where $Pa(y_i)$ is a subset of $Y \setminus \{y_i\}$ and $k_i \in K$.

Intuitively, an SCM can be thought of representing causal relationships in a system as a directed acyclic graph (DAG), where variables are represented as nodes and causal relationships between them are represented as edges. Variables are distinguished as endogenous or exogenous based on whether or not (respectively) they are affected by other variables in the system.

We interpret a neural network-based deepfake detector as an SCM to analyze the relationship between its neurons and predictions.

Definition 2 (Deepfake detector as an SCM). A deepfake detection model $N(y_1, y_2, \dots, y_n)$ is interpreted as an SCM by the four-tuple $C([y_1, y_2, \dots, y_n], K, [f_1, f_2, \dots, f_n], P_k)$, where y_i is the set of network neurons at layer i , y_1 and y_n are the neurons at input and output layers respectively, K is a set of exogenous random variables to serve as causal factors for input-layer neurons x_1 , and P_k is a probability distribution over K . Corresponding to each y_i , f_i is the set of causal functions for the neurons at layer i .

Figure 4 illustrates a deepfake detection model interpreted as an SCM. Here, the solid-line neurons correspond to endogenous variables, whereas the dotted circles represent the latent exogenous noise variables which serve as causal factors for input neurons. Functions connect the layers, with edge weights corresponding to the cause-effect relations. Note that the input layer neurons can be denoted as the functions of the latent

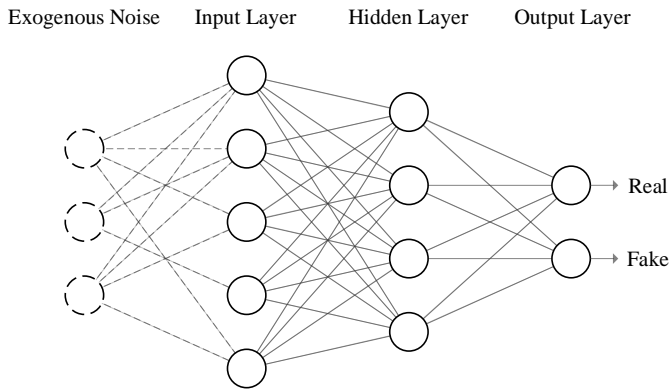


Fig. 4: Interpretation of a deepfake detector neural network as an SCM

exogenous variables, and are assumed not causally related to each other (but can be jointly affected by latent noise).

Finally, we need a measure of each neuron’s contribution to the generalizability of a detector, which we based on the average causal effect in the SCM representation:

Definition 3 (Average Causal Effect (ACE)). Let y denote a neuron of a neural network-based deepfake detector N and z denote the measure of N ’s degradation (as described in Sections IV-A–IV-B). Then, the *average causal effect (ACE)* of y on z is:

$$ACE_{do(y=\gamma)}^z = \mathbb{E}[z|do(y = \gamma)] = \int_z zp(z|do(y = \gamma))dz,$$

where $do(\cdot)$ is the corresponding interventional distribution defined by SCM, and $ACE_{do(y=\gamma)}^z$ is calculated by the interventional exception of z given $do(y = \gamma)$.

Specifically, given a deepfake detector N , we sample input x from an unseen dataset U and denote $N_{ac}(x)$ as N ’s predicted class corresponding to x ’s ground-truth label $L(x)$. For each neuron y , we keep $y = \gamma$ and measure its contribution to z by calculating $ACE_{do(y=\gamma)}^{N_{ac}(x)}$ with the sampled inputs.

Ultimately, by calculating the causal effect of each neuron in N (based on the testing samples in U), i.e., their contributions to N ’s generalization, the contributing neurons are identified.

Experiment. Based on the above, we applied a causality analysis on the deepfake detectors implemented in Section III-C in order to identify neurons contributing to both seen and unseen datasets (and thus may potentially be involved with generalizable features). Specifically, we identify the contributing neurons in the first dense layer of the `MesoNet`, `MesoInception`, and `ShallowNet` detectors, since such layers receive significant features extracted by Conv modules and conduct actual classification functions [33]. `XceptionNet` and `EfficientNet` are not selected since they both contain only one dense layer that is augmented to perform binary classification, and thus their dense layers contain limited numbers of neurons that are not enough to analyze and compare contributions. (We will further discuss the limitations on unselected detectors in Section VI.)

In our experiment, based on the five datasets containing the detectors’ original testing images as well as the four unseen datasets, we identified the top 64, 128, 256, and 512 contributing neurons in the detectors’ first dense layers (1024 neurons in total; thus the top 1/16, 1/8, 1/4, and 1/2 respectively). Following the causality analyses, we then counted the number of ‘overlapping’ neurons (i.e., the contributing neurons involved across multiple datasets) and the number of datasets they contributed to a decision in, up to a total of 5 times (CELEBV2, FS, NT, DF, and DFD).

Results. We present our results in Figure 5, where each histogram presents the outcome of a causality analysis on one deepfake detector. For example, in Figure 5 (a), when identifying the top 64 contributing neurons `MesoNet1`, we can see that 42 of them contributed to classification for all five testing datasets (CELEBV2, FS, NT, DF, and DFD), whereas, for example, 21 of them only contributed to the decision for one of the five datasets.

As can be seen by the green columns in these histograms, we observe that neurons were most frequently contributing to *all five datasets*, regardless of whether considering the top 64, 128, 256, or 512 neurons. This was especially the case for the last of the categories. For example, when analyzing `MesoNet1` in Figure 5 (a), 407 neurons (out of the top 512) were identified as contributing to the decision across all five datasets. The exception cases are shown in Figures 5 (m) and (p): when identifying the top-64 and top-128 contributing neurons in these `ShallowNet` detectors, we do not observe a significant number of neurons contributing across all five datasets in comparison to the other frequencies. However, when considering the top 256 or 512 contributing neurons, their results are consistent with other detectors. Such results are reasonable since deepfake detectors might make unstable decisions based on the features involved in only 64 or 128 neurons. In general, however, the results suggest that there are neurons that are universally contributing to the detection of both the original and unseen testing datasets, which may provide a useful basis for building generalizable deepfake detectors in the future.

Contrast this with our observations in Section IV-C (RQ3), in which we found that deepfake detectors extracted unrestrained features from inputs. Our causality-based analysis took a more granular view of the neural networks and observed that across all the detectors, it is possible to identify neurons that contribute to the decision across all five unseen datasets. Thus, we conjecture that detectors focusing on these universally contributing neurons may be more successful at generalizing to different datasets.

Discussion. Existing efforts have provided some inspiration for making use of important neurons in neural networks, such as pruning those low-contributing neurons and then fine-tuning them or enhancing models based on transfer learning [59]. However, applying these strategies to deepfake detection still has a long way to go, since the variety of deepfake datasets can lead to various potential risks, such as overfitting, catastrophic forgetting [60], or performance degradation due to the reduction of network parameters. Despite this, compared with existing generalization methods (Section II-C) that mainly



Fig. 5: Causality analysis: the number of (overlapping) neurons that have contributed to classification across the five testing datasets (CELEBV2, F'S, NT, DF, and DFD)

focus on fine-tuning deepfake detectors at layer levels, our results suggest a granular neuron-level optimization may have greater potential for achieving generalizable deepfake detection.

Finding 4: Neural network deepfake detectors have universally contributing neurons across seen/unseen datasets.

V. RESEARCH DIRECTIONS

In this section, we discuss and recommend potential research directions based on the conclusions from our empirical study. *Building deepfake detectors based on causality analysis.* Based on our studies in Section IV-D (RQ4), through causality analysis, we can identify the contributing neurons that may in-

volve meaningful features for generalizability. Thus, a prospective research direction is to build deepfake detectors based on those universal contributing neurons. For example, when training deepfake detectors, we might increase the weights of the universally contributing neuron-related parameters or freeze the remaining, low-contributing neurons. As we discussed in the concluding paragraph of Section IV-D, applying causality analysis to achieve generalizable deepfake detection still has a long way to go. Fortunately, we have taken the first step of demonstrating the existence of these universally contributing neurons, the use of which should be explored in future research.

Preventing deepfake detectors from learning interferential features. Based on our findings in Section IV-B (RQ2) and Section IV-C (RQ3), deepfake detectors have learned unwanted synthesis-method properties, and extract unrestrained features that are not discriminative enough for generalization. These findings indicate a potential research direction, i.e., applying certain measures to prevent detectors from learning interferential properties, such as applying *Dropout* [61] operations supplementing regularization terms in loss functions [62], so as to enable detectors to focus on those truly meaningful features.

Evaluating upcoming deepfake detectors. To perform our study, we created a repository of deepfake detectors as well as datasets in multiple settings. Based on our studies in Section IV-A (RQ1), the generalization problem is common across deepfake detectors. Therefore, our implemented deepfake detectors and datasets can serve as baselines to evaluate whether an upcoming deepfake detector is reliably generalizable.

VI. THREATS TO VALIDITY

In this section, we will discuss potential threats to the validity of our empirical study.

External validity: limitation of the proposed causality analysis method. In Section IV-D (RQ4), we performed causality analyses on the dense layers of MesoNet, MesoInception, and ShallowNet. Although our proposed method applies to multiple deepfake detectors, it is not enough to analyze those detectors with only one or without any dense layers, such as XceptionNet and EfficientNet, since such layers contain limited neurons for binary classification and it makes no sense to analyze such neurons. In this RQ, our aim is to explore the possibility towards generalizable detection, and the potential neurons have been found from these used detectors. Thus, although the proposed causality analysis method could still be improved, our existing explorations meet the goal of this study.

Internal validity: selection of deepfake detectors. We have selected multiple state-of-the-art deep learning-based deepfake detectors (Section II-B). Although specific feature-based detectors also report some promising results (mainly on seen datasets), they are not suitable for generalizability studies due to their instability (limited by objective factors). Moreover, such detectors are still in the early stages of being applied in practice. Our selected deep learning-based detectors are most likely to generalize and are thus most suitable for this study.

Construct validity: implementation of deepfake detectors. We have trained multiple deepfake detectors (Section III-C)

whose performance can potentially be affected by their implementations, such as optimizer or learning rates. To mitigate such concerns, we implemented these detectors based on the settings that have been evaluated by their original authors or related effective implementations. Moreover, we have evaluated these detectors and observed promising original accuracy, and thus they meet the requirements to perform this study.

VII. CONCLUSION

In this work, we conducted an empirical study to systematically explore how generalizable deepfake detectors are. Based on our studies, we have: (1) confirmed that existing deepfake detectors lack generalizability, especially in zero-shot settings; (2) found that deepfake detectors learn unwanted method-specific and unrestrained features that are not discriminative for generalization; and (3) proposed a causality analysis method that identifies the presence of universally contributing neurons across unseen datasets, which may open a path forward to solving the generalizability problem. Finally, we have provided a repository of our deepfake detectors and datasets, which we believe can provide baselines for evaluating the generalizability of new deepfake detection approaches.

REFERENCES

- [1] R. Tolosana, R. Vera-Rodriguez, J. Fierrez, A. Morales, and J. Ortega-Garcia, "Deepfakes and beyond: A survey of face manipulation and fake detection," *Information Fusion*, vol. 64, pp. 131–148, 2020.
- [2] C. Li, L. Wang, S. Ji, X. Zhang, Z. Xi, S. Guo, and T. Wang, "Seeing is living? rethinking the security of facial liveness verification in the deepfake era," *CoRR abs/2202.10673*, 2022.
- [3] F. Matern, C. Riess, and M. Stamminger, "Exploiting visual artifacts to expose deepfakes and face manipulations," in *2019 IEEE Winter Applications of Computer Vision Workshops (WACVW)*. IEEE, 2019, pp. 83–92.
- [4] Z. Gu, Y. Chen, T. Yao, S. Ding, J. Li, F. Huang, and L. Ma, "Spatiotemporal inconsistency learning for deepfake video detection," in *Proceedings of the 29th ACM international conference on multimedia*, 2021, pp. 3473–3481.
- [5] H. Liu, X. Li, W. Zhou, Y. Chen, Y. He, H. Xue, W. Zhang, and N. Yu, "Spatial-phase shallow learning: rethinking face forgery detection in frequency domain," in *Proceedings of the IEEE/CVF conference on computer vision and pattern recognition*, 2021, pp. 772–781.
- [6] Y. Li, X. Yang, P. Sun, H. Qi, and S. Lyu, "Celeb-df: A large-scale challenging dataset for deepfake forensics," in *Proceedings of the IEEE/CVF conference on computer vision and pattern recognition*, 2020, pp. 3207–3216.
- [7] D. Afchar, V. Nozick, J. Yamagishi, and I. Echizen, "Mesonet: a compact facial video forgery detection network," in *2018 IEEE international workshop on information forensics and security (WIFS)*. IEEE, 2018, pp. 1–7.
- [8] F. Chollet, "Xception: Deep learning with depthwise separable convolutions," in *Proceedings of the IEEE conference on computer vision and pattern recognition*, 2017, pp. 1251–1258.
- [9] D. Cozzolino, J. Thies, A. Rössler, C. Riess, M. Nießner, and L. Verdoliva, "Forensictransfer: Weakly-supervised domain adaptation for forgery detection," *arXiv preprint arXiv:1812.02510*, 2018.
- [10] H. H. Nguyen, F. Fang, J. Yamagishi, and I. Echizen, "Multi-task learning for detecting and segmenting manipulated facial images and videos," in *2019 IEEE 10th International Conference on Biometrics Theory, Applications and Systems (BTAS)*. IEEE, 2019, pp. 1–8.
- [11] M. Kim, S. Tariq, and S. S. Woo, "Cored: Generalizing fake media detection with continual representation using distillation," in *Proceedings of the 29th ACM International Conference on Multimedia*, 2021, pp. 337–346.
- [12] S. Lee, S. Tariq, J. Kim, and S. S. Woo, "Tar: Generalized forensic framework to detect deepfakes using weakly supervised learning," in *IFIP International Conference on ICT Systems Security and Privacy Protection*. Springer, 2021, pp. 351–366.

- [13] M. Kim, S. Tariq, and S. S. Woo, "Fretal: Generalizing deepfake detection using knowledge distillation and representation learning," in *Proceedings of the IEEE/CVF conference on computer vision and pattern recognition*, 2021, pp. 1001–1012.
- [14] K. Sun, H. Liu, Q. Ye, Y. Gao, J. Liu, L. Shao, and R. Ji, "Domain general face forgery detection by learning to weight," in *Proceedings of the AAAI conference on artificial intelligence*, vol. 35, no. 3, 2021, pp. 2638–2646.
- [15] M. Du, S. Pentylala, Y. Li, and X. Hu, "Towards generalizable deepfake detection with locality-aware autoencoder," in *Proceedings of the 29th ACM International Conference on Information & Knowledge Management*, 2020, pp. 325–334.
- [16] L. Chen, Y. Zhang, Y. Song, L. Liu, and J. Wang, "Self-supervised learning of adversarial example: Towards good generalizations for deepfake detection," in *Proceedings of the IEEE/CVF Conference on Computer Vision and Pattern Recognition*, 2022, pp. 18 710–18 719.
- [17] S. Tariq, S. Lee, and S. Woo, "One detector to rule them all: Towards a general deepfake attack detection framework," in *Proceedings of the Web Conference 2021*, 2021, pp. 3625–3637.
- [18] Y. Xu, K. Raja, and M. Pedersen, "Supervised contrastive learning for generalizable and explainable deepfakes detection," in *Proceedings of the IEEE/CVF Winter Conference on Applications of Computer Vision*, 2022, pp. 379–389.
- [19] A. Rossler, D. Cozzolino, L. Verdoliva, C. Riess, J. Thies, and M. Nießner, "Faceforensics++: Learning to detect manipulated facial images," in *Proceedings of the IEEE/CVF International Conference on Computer Vision*, 2019, pp. 1–11.
- [20] V. Badrinarayanan, A. Kendall, and R. Cipolla, "Segnet: A deep convolutional encoder-decoder architecture for image segmentation," *IEEE transactions on pattern analysis and machine intelligence*, vol. 39, no. 12, pp. 2481–2495, 2017.
- [21] I. Goodfellow, J. Pouget-Abadie, M. Mirza, B. Xu, D. Warde-Farley, S. Ozair, A. Courville, and Y. Bengio, "Generative adversarial nets," in *Advances in neural information processing systems*, 2014, pp. 2672–2680.
- [22] J. Thies, M. Zollhofer, M. Stamminger, C. Theobalt, and M. Nießner, "Face2face: Real-time face capture and reenactment of rgb videos," in *Proceedings of the IEEE conference on computer vision and pattern recognition*, 2016, pp. 2387–2395.
- [23] J. Thies, M. Zollhöfer, and M. Nießner, "Deferred neural rendering: Image synthesis using neural textures," *ACM Transactions on Graphics (TOG)*, vol. 38, no. 4, pp. 1–12, 2019.
- [24] P. Isola, J.-Y. Zhu, T. Zhou, and A. A. Efros, "Image-to-image translation with conditional adversarial networks," in *Proceedings of the IEEE conference on computer vision and pattern recognition*, 2017, pp. 1125–1134.
- [25] R. Rombach, A. Blattmann, D. Lorenz, P. Esser, and B. Ommer, "High-resolution image synthesis with latent diffusion models," in *Proceedings of the IEEE/CVF Conference on Computer Vision and Pattern Recognition*, 2022, pp. 10 684–10 695.
- [26] P. Korshunov and S. Marcel, "Deepfakes: a new threat to face recognition? assessment and detection," *arXiv preprint arXiv:1812.08685*, 2018.
- [27] X. Yang, Y. Li, and S. Lyu, "Exposing deep fakes using inconsistent head poses," in *ICASSP 2019-2019 IEEE International Conference on Acoustics, Speech and Signal Processing (ICASSP)*. IEEE, 2019, pp. 8261–8265.
- [28] Y. Li and S. Lyu, "Exposing deepfake videos by detecting face warping artifacts," *arXiv preprint arXiv:1811.00656*, 2018.
- [29] S. Agarwal, H. Farid, Y. Gu, M. He, K. Nagano, and H. Li, "Protecting world leaders against deep fakes," in *CVPR workshops*, vol. 1, 2019, p. 38.
- [30] H.-S. Chen, M. Rouhsedaghat, H. Ghani, S. Hu, S. You, and C.-C. J. Kuo, "Defakehop: A light-weight high-performance deepfake detector," in *2021 IEEE International Conference on Multimedia and Expo (ICME)*. IEEE, 2021, pp. 1–6.
- [31] S. Tariq, S. Lee, H. Kim, Y. Shin, and S. S. Woo, "Gan is a friend or foe? a framework to detect various fake face images," in *Proceedings of the 34th ACM/SIGAPP Symposium on Applied Computing*, 2019, pp. 1296–1303.
- [32] M. Tan and Q. Le, "Efficientnet: Rethinking model scaling for convolutional neural networks," in *International conference on machine learning*. PMLR, 2019, pp. 6105–6114.
- [33] K. O'Shea and R. Nash, "An introduction to convolutional neural networks," *arXiv preprint arXiv:1511.08458*, 2015.
- [34] C. Szegedy, W. Liu, Y. Jia, P. Sermanet, S. Reed, D. Anguelov, D. Erhan, V. Vanhoucke, and A. Rabinovich, "Going deeper with convolutions," in *Proceedings of the IEEE conference on computer vision and pattern recognition*, 2015, pp. 1–9.
- [35] C. Aaron, "Dfdetect," <https://deepfake-detect.com>, accessed on 10 April 2023.
- [36] C. Vaccari and A. Chadwick, "Deepfakes and disinformation: Exploring the impact of synthetic political video on deception, uncertainty, and trust in news," *Social Media+ Society*, vol. 6, no. 1, p. 2056305120903408, 2020.
- [37] D. Gamage, J. Chen, P. Ghasiya, and K. Sasahara, "Deepfakes and society: What lies ahead?" in *Frontiers in Fake Media Generation and Detection*. Springer, 2022, pp. 3–43.
- [38] M. Appel and F. Prietzel, "The detection of political deepfakes," *Journal of Computer-Mediated Communication*, vol. 27, no. 4, p. zmac008, 2022.
- [39] B. Zhao, S. Zhang, C. Xu, Y. Sun, and C. Deng, "Deep fake geography? when geospatial data encounter artificial intelligence," *Cartography and Geographic Information Science*, vol. 48, no. 4, pp. 338–352, 2021.
- [40] Z. Liu, X. Qi, and P. H. Torr, "Global texture enhancement for fake face detection in the wild," in *Proceedings of the IEEE/CVF conference on computer vision and pattern recognition*, 2020, pp. 8060–8069.
- [41] T. Yang, Z. Huang, J. Cao, L. Li, and X. Li, "Deepfake network architecture attribution," *arXiv preprint arXiv:2202.13843*, 2022.
- [42] A. Rossler, "Faceforensics github repository," <https://github.com/ondyari/FaceForensics>, accessed on 10 April 2023.
- [43] D. Nick and G. Andrew, "Google research blog. contributing data to deepfake detection research," <https://ai.googleblog.com/2019/09/contributing-data-to-deepfake-detection.html>, accessed on 10 April 2023.
- [44] L. Yuezun, "celeb-deepfakeforensics github repository," <https://github.com/yuezunli/celeb-deepfakeforensics>, accessed on 10 April 2023.
- [45] Y. Li, X. Yang, P. Sun, H. Qi, and S. Lyu, "Celeb-df (v2): a new dataset for deepfake forensics," *arXiv preprint arXiv:1909.12962*, 2019.
- [46] A. Chattopadhyay, P. Manupriya, A. Sarkar, and V. N. Balasubramanian, "Neural network attributions: A causal perspective," in *International Conference on Machine Learning*. PMLR, 2019, pp. 981–990.
- [47] M. Tan, B. Chen, R. Pang, V. Vasudevan, M. Sandler, A. Howard, and Q. V. Le, "Mnasnet: Platform-aware neural architecture search for mobile," in *Proceedings of the IEEE/CVF conference on computer vision and pattern recognition*, 2019, pp. 2820–2828.
- [48] F. Zhuang, Z. Qi, K. Duan, D. Xi, Y. Zhu, H. Zhu, H. Xiong, and Q. He, "A comprehensive survey on transfer learning," *Proceedings of the IEEE*, vol. 109, no. 1, pp. 43–76, 2020.
- [49] Ageitgey, "Face_recognition github repository," https://github.com/ageitgey/face_recognition, accessed on 10 April 2023.
- [50] D. P. Kingma and J. Ba, "Adam: A method for stochastic optimization," *arXiv preprint arXiv:1412.6980*, 2014.
- [51] R. R. Selvaraju, M. Cogswell, A. Das, R. Vedantam, D. Parikh, and D. Batra, "Grad-cam: Visual explanations from deep networks via gradient-based localization," in *Proceedings of the IEEE international conference on computer vision*, 2017, pp. 618–626.
- [52] Y. Zhang, P. Tiño, A. Leonardis, and K. Tang, "A survey on neural network interpretability," *IEEE Transactions on Emerging Topics in Computational Intelligence*, 2021.
- [53] R. Meudec, "tf-explain github repository," <https://github.com/sicara/tf-explain>, accessed on 10 April 2023.
- [54] G. Bradski, "The opencv library," *Dr. Dobbs's Journal: Software Tools for the Professional Programmer*, vol. 25, no. 11, pp. 120–123, 2000.
- [55] Z. Wang, A. C. Bovik, H. R. Sheikh, and E. P. Simoncelli, "Image quality assessment: from error visibility to structural similarity," *IEEE transactions on image processing*, vol. 13, no. 4, pp. 600–612, 2004.
- [56] B. Sun, J. Sun, L. H. Pham, and J. Shi, "Causality-based neural network repair," in *Proceedings of the 44th International Conference on Software Engineering*, 2022, pp. 338–349.
- [57] Q. Zhao and T. Hastie, "Causal interpretations of black-box models," *Journal of Business & Economic Statistics*, vol. 39, no. 1, pp. 272–281, 2021.
- [58] J. Pearl, *Causality*. Cambridge university press, 2009.
- [59] P. Molchanov, S. Tyree, T. Karras, T. Aila, and J. Kautz, "Pruning convolutional neural networks for resource efficient inference," *arXiv preprint arXiv:1611.06440*, 2016.
- [60] R. Kemker, M. McClure, A. Abitino, T. Hayes, and C. Kanan, "Measuring catastrophic forgetting in neural networks," in *Proceedings of the AAAI conference on artificial intelligence*, vol. 32, no. 1, 2018.
- [61] N. Srivastava, G. Hinton, A. Krizhevsky, I. Sutskever, and R. Salakhutdinov, "Dropout: a simple way to prevent neural networks from overfitting," *The journal of machine learning research*, vol. 15, no. 1, pp. 1929–1958, 2014.
- [62] X. Ying, "An overview of overfitting and its solutions," in *Journal of physics: Conference series*, vol. 1168. IOP Publishing, 2019, p. 022022.